Study of $LiFePO_4$ Electrode Morphology for Li-Ion Battery Performance

MIHAELA BUGA*, ALEXANDRU RIZOIU, CONSTANTIN BUBULINCA, SILVIU BADEA, MIHAI BALAN, ALEXANDRU CIOCAN, ALIN CHITU

National R&D Institute for Cryogenic and Isotopic Technologies ICIT, 4 Uzinei Str., 240050, Ramnicu Valcea, Romania

The paper focuses on the development of lithium-ion battery cathode based on lithium iron phosphate ($LiFePO_4$). Li-ion battery cathodes were manufactured using the new Battery R&D Production Line from ROM-EST Centre, the first and only facility in Romania, capable of fabricating the industry standard 18650 lithium-ion cells, customized pouch cells and CR2032 cells. The cathode configuration contains acetylene black (AB), $LiFePO_4$, polyvinylidene fluoride (PVdF) as binder and N-Methyl-2-pyrrolidone (NMP) as solvent. X-ray diffraction measurements and SEM-EDS analysis were conducted to obtain structural and morphological information for the as-prepared electrodes.

Keywords: lithium-ion battery, $LiFePO_4$, roll-to-roll, electrode morphology

Considered close to become state-of-the-art technology for a range of advanced electrochemical energy storage and conversion systems, Li-ion batteries are promising candidates as power sources for portable devices and automotive industry, as well as for large-scale energy storage applications in conjunction with renewable energy sources [1-3]. Whether intended for mobile or stationary applications, it is, however, highly desirable to improve the energy storage capacity together with life cycle performance by keeping the capital cost low and maintaining the system stability high [4-6]. When it comes to safety, Li-ion batteries can be dangerous under some conditions since they contain, unlike other rechargeable batteries, a flammable electrolyte kept pressurized [7-9]. Chemistry, performance, cost and safety characteristics vary across Li-ion battery types. For instance, $LiCoO_2$ are commonly used with portable devices (e.g., cell phones, handy-cameras and laptops) and exhibit high energy storage density at the expense of safety issues, especially when damaged [10-12]. On the other hand, olivine-type $LiFePO_4$, is a desirable cathode material with outstanding features, such as low cost, superior thermal stability, enhanced safety, high theoretical specific capacity (170 $mAh \cdot g^{-1}$) and suitable charge/discharge voltage plateau (3.45V vs. Li) [13-15]. However, the slow rate of lithium ion diffusion, poor electronic and ionic conductivities [16], restricts its rate capability and electrochemical performance, particularly for high power applications. Additionally, the composition, homogeneity and thickness of the electrodes play a crucial role as they consist of an active material, binders (e.g., PVdF) and conductive agents (e.g., carbon powders) which are mixed in certain proportions and are compacted into porous layers (i.e., with porosities between 30% and 40%) under inert atmosphere (e.g., Ar gas).

In this paper, we report the roll-to-roll processing technology for the preparation of $LiFePO_4$ cathodes. Electrodes surface morphology was confirmed by SEM analysis coupled to an auxiliary EDS detector. X-Ray Diffraction results reveal the single-phase and perfectly crystalline structure. A transfer of this cathode concept is dedicated to future research in order to understand the overall performance of the $LiFePO_4$ batteries.

Experimental part

Materials and methods

Commercially available battery grade cathode material - Lithium iron phosphate ($LiFePO_4$) (LFPO) powder and acetylene black powder were purchased from MTI Corp.; Polyvinylidene fluoride (PVdF)-SOLEF 5130 used as a binder was purchased from Solvay; N-methyl-2-pyrrolidone (NMP, ≥ 99.0%) from Sigma-Aldrich; aluminium foil (20 µm thick) were supplied from Custom Cells. All reagents were used without further purification or treatment. PVdF was dissolved in NMP at 40°C under stirring.

Processing route

The processing route implies powder and slurry mixing, electrode film coating and drying, electrode calendering and cutting. A cathode slurry of required consistency was prepared by mixing active material powder (LFPO 90 wt.%.), conductive agent (AB 5wt.%) and 5 wt.% PVdF dissolved in NMP, using a high dispersing and vacuum mixer for approximately 3 h. In order to guarantee good slurry homogeneity and exclude any particle agglomerates, a highly concentrated suspension was initially mixed, while the amount of NMP was raised stepwise with time. Any cluster formation in the following coating step restricts the electrical and mechanical properties of the electrodes. The resulted slurry (fig. 1 a) was subsequently coated on

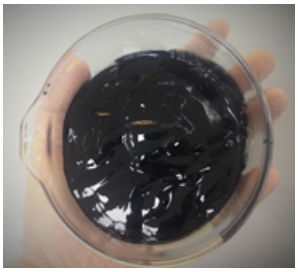

a

b

Fig. 1. A ready-to-coat cathode slurry (a); roll-to-roll processing technology using the semi-automatic electrode coating machine – intermittent coating (b)

* email: mihaela.buga@icsi.ro

aluminium foil (thickness: 20μm) by roll-to-roll processing technology using the semi-automatic electrode coating machine. From the coater part, the coated foil was fed directly into a drying oven (to bake the electrode material onto the foil and to evaporate the solvent), then dry electrode roller was obtained (fig. 1 b). In this step, in order to obtain a uniform and defect-free film, some operating coating parameters are mandatory (clean operation – low contamination of the coating layer, the coating speed, the stability of the coating bead, the drying temperature and the transit time through the oven).

In order to increase the energy density, the electrodes were calendered, decreasing the electrode porosity to approximately 20-40%. The electrodes thickness was reduced to a controlled value by driving them through two massive cylindrical rolls under large pressure and adjustable rolling speed. The electrodes porosity plays an important role allowing a good contact between the particles and the electrolyte and a large surface area available for the electrochemical reactions. In the same time, compacting the electrode structure also increases its adhesion to current collector foil, and decreases the resistivity. The overall length of roll-to-roll processed raw-electrodes is far larger than the dimensions of the future CR2032 Li-ion coin cells (meaning 20 mm in diameter and 3.2 mm in height). Thus, several series of coin electrodes were obtained by punching the dried electrodes into discs of 16 mm in diameter (fig. 2). After this operation the electrodes were dried to remove all water contamination followed by weigh. Also, in order to verity the uniformity, the thickness was measured by micrometer. Several series of uncalendared and uncoated electrodes of the same aluminium foil (discs of 16 mm) were obtained, weight and measured by micrometer.

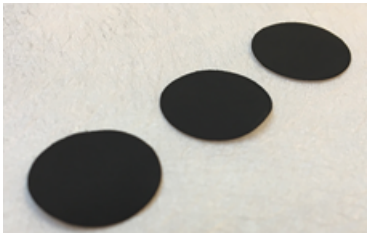

Fig. 2. Optical photograph of the produced $LiFePO_4$ cathodes (discs of 16 mm)

Morphological information including internal structure was obtained through the scanning electron microscopy analysis of the electrodes. The analysis has been performed using a FE-SEM VP device made by CARL ZEISS, equipped with an X-ray energy dispersive spectrometer (EDS). Quantitative surface metrology with nanometer-level precision with superior gage capability and high resolution 1 million pixel image sensor providing fast areal measurements in seconds, for excellent surface detail and visualization were obtained using ZeGage 3D Optical Surface Profiler manufactured by Zygo. This unit is a portable profile scanners and it can produce results fast, reliable and with grate accuracy. Some of the advantages of the Zygo optical profiler are that it runs a proprietary non-contact measurement technology that has low sensitivity to vibration effects, eliminating the need for vibration isolation platforms in most applications.

XRD patterns were obtained using a BRUKER-RIGAKU MiniFlex600 diffractometer with CuKα radiation and 40 kV tube voltage.

Results and discussions

Macroscopically homogenous cathodes were obtained with a shiny aspect for the calendared electrode compared to the uncalendared electrode that appeared matte black. Typical SEM images for both uncalendared and calendared electrode are shown in figure 3.

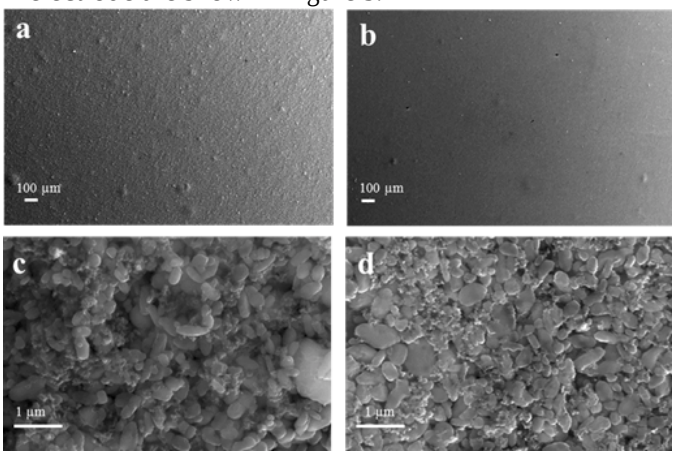

Fig.3. SEM images of (a, c) uncalendared electrode and calendared electrode (b, d) at different magnification

SEM micrographs at different magnification are presented, showing highly porous structures, crack-free and stable coating throughout the electrode surface with small differences between the thicknesses of the coated layers. Also, the SEM images of the calendared electrode show a reduction in porosity after electrode densification. On the other hand, small defects can also be detected. The defects on the electrode are associated with the binder shrinkage during the final drying step and with the particle size of acetylene black which is not uniformly distributed, due to the broad particle-size distribution.

Figure 4 shows the cross-section images of both as-coated and calendered cathode electrodes. A significant difference is visible between the as-coated (40 μm) and calendered electrodes (30 μm) in the SEM images. The SEM images 3a) and 3b) clearly show that the pores shrink in size and electrodes are well compacted after calendering in comparison to the as-coated electrodes.

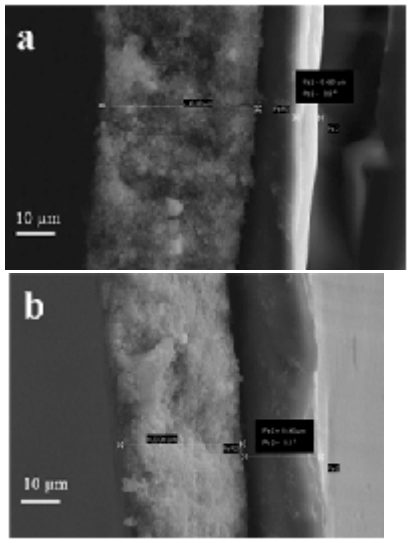

Fig. 4. Cross-section SEM images of the as coated $LiFePO_4$ cathode (a) and calendered $LiFePO_4$ cathode (b)

SEM imaging and EDS elemental mapping of large surface areas indicate that the chemical composition is uniformly distributed along the porous electrodes and in cross-section, whereas the structural properties and stoichiometry are similar to those of the precursors used (i.e., commercially available powders). SEM images with the corresponding EDS spectrum and EDS mapping images for both as-coated and calendered cathodes are presented in figure 5 and 6.

As shown in figure 6 EDS spectrum, there is trace amount of Mn detected by EDS in the calendered $LiFePO_4$

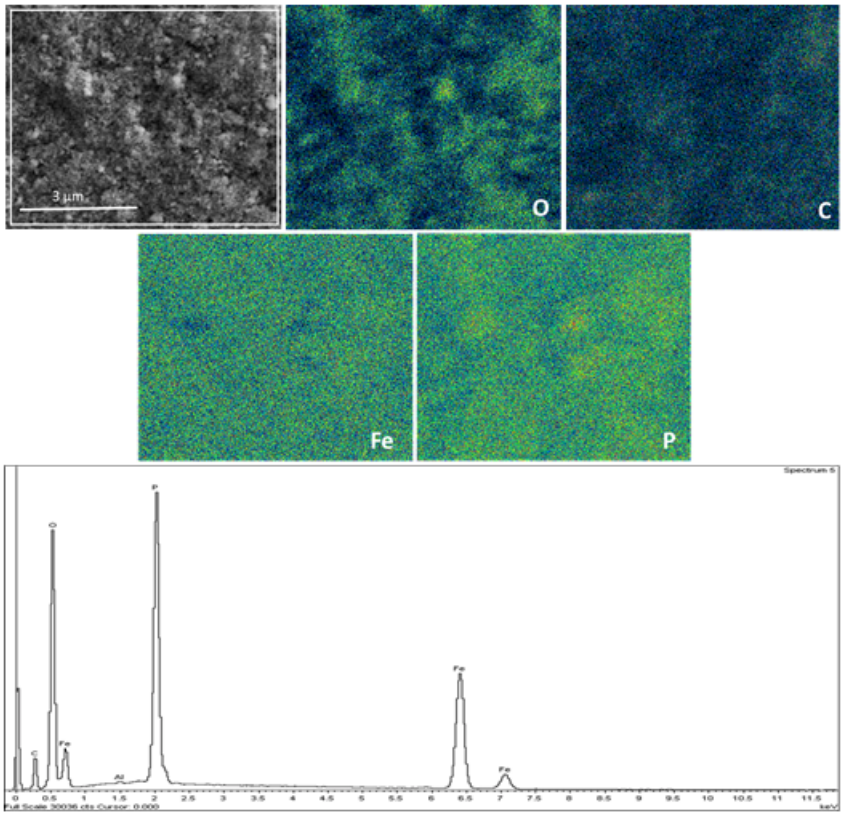

Fig. 5. SEM image of as coated $LiFePO_4$ cathode; EDS elemental mapping images of O, C, Fe and P; EDS spectrum

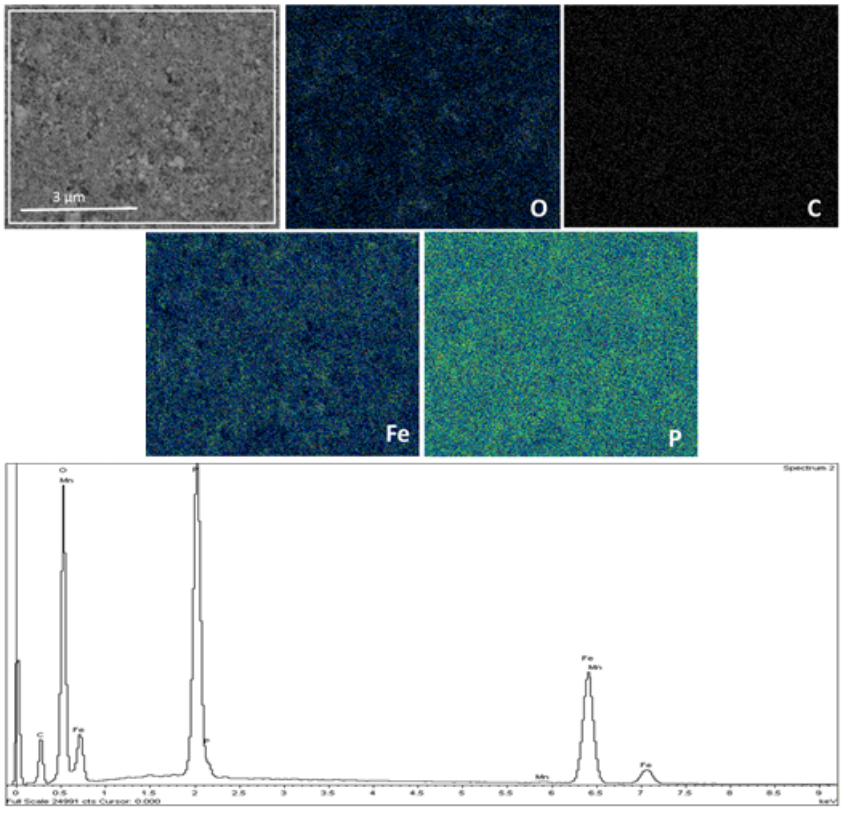

Fig. 6. SEM image of calendered $LiFePO_4$ cathode; EDS elemental mapping images of O, C, Mn, Fe and P; EDS spectrum

cathode sample. This could be due to contamination during EDS sample measurement, or electrode calendering process.

In figure 7, we can observe the optical profile of as coated $LiFePO_4$ cathode rolled onto an aluminium foil.

One can observe that the overall pressing process is homogenous and that the average height peak of the obtained layer is 0.752µm. We can also see there the high and low spots are located and by using a stitching technique we can create a bigger profile for better understanding of

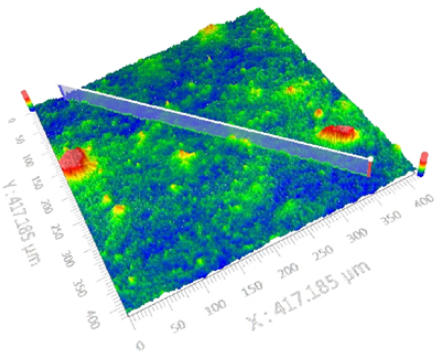

Fig. 7. Optical profile of as coated $LiFePO_4$ cathode rolled onto aluminium foil

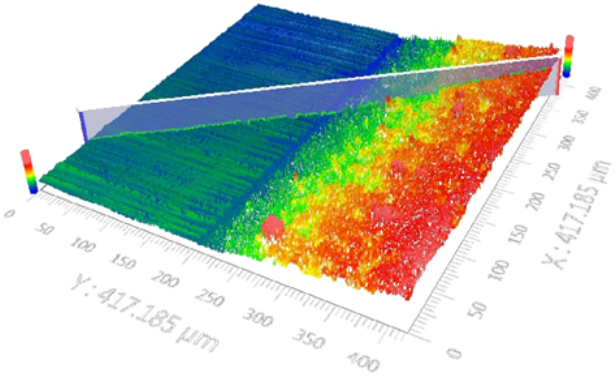

Fig. 8. Optical profile of as coated $LiFePO_4$ cathode rolled onto aluminium foil of the start of the rolling process

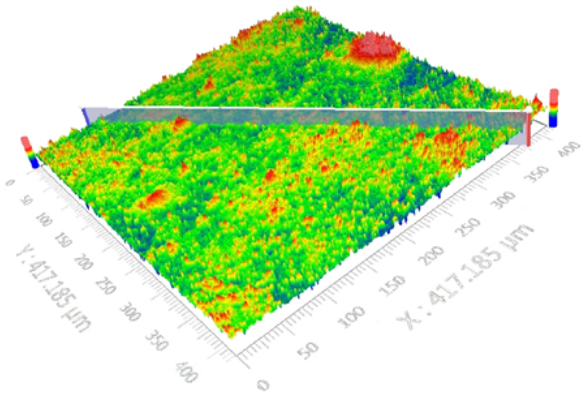

Fig. 9. Optical profile of calendered $LiFePO_4$ cathode rolled onto aluminium foil

the behaviour of the whole cell. The scanned are, although small, gives us great information about the rolling process right from the beginning. You can determine whether you have a good electrode material to work with or if the rolling machine is well calibrated.

In figure 8, we have a complete look of the start of the rolling process. Of the left of the image, we have the bare aluminium foil and half way through we can see the start of the electrode material layer. We can determine that the rolling equipment is well calibrated because of the even and gradually started deposition. Also, using this technology you can have an idea on the aluminium foil used for electrodes.

In figure 9 we have the pressed electrode. From this image we can determine the way that the electrode has been pressed. Engaging in this kind of analysis we can adjust very precisely the thickness of the deposed layer. Here we can see that the lowest point measured is -0.913µm and the highest point is rated at 1.063µm.

The powder X-ray diffraction pattern (XRD) taken from the as-coated cathodes is shown in figure 10. All presented peaks could be indexed to an orthorhombic system of olivine-type structure P_{nma} space group (ICDD PDF No. 62) [17] with lattice constant parameter a=6.014103, b=10.335331 and c=4.695588. The profiles shows good agreement with the theoretical data, confirming the presence of $LiFePO_4$ as a single crystalline phase in the final powder.

This is also supported by Williamson - Hall analysis that yields a relatively low value for the average crystallite-size (i.e., ~ 855Å) and high deformation strain (i.e., ~0.002%).

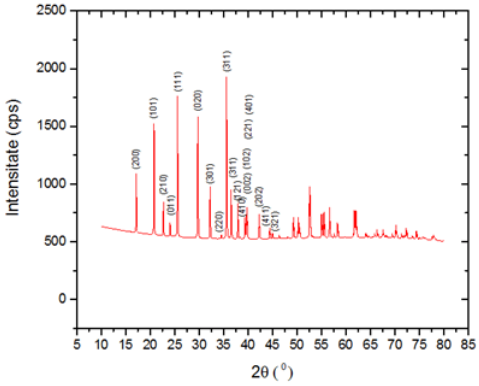

Fig. 10. XRD patterns obtained for $LiFePO_4$ electrodes and peak positions corresponding to Miller indices.

Conclusions

In summary, we have successfully prepared Li-ion battery cathodes based on lithium iron phosphate *via* roll-to-roll processing technology with the active material loading for the $LiFePO_4$ electrodes of 6.75 mg/cm^2 on a specific active area of 2.0096 cm^2. In order to understand the overall performance of the CR2032 batteries based on $LiFePO_4$ cathodes, further work is being focused on recording impedance spectroscopy, capacity retention and lifetime tests at various charge/discharge rate capacity values.

Acknowledgements: Thanks to Nicu Becherescu from Apel Laser, for the electrode surface details obtained by ZeGage 3D Optical Surface Profiler-Zygo.

References

1.SCROSATI, B., GARCHE, J., Journal of Power Sources, **195**, 2010, p. 2419-2430
2.*** http://www.sandia.gov/ess/docs/other/Grid_Energy_Storage_Dec_2013.pdf, Last access: 10.07.2017
3.SHOKRZADEH, S., BIBEAU, E., Energy, **106**, 2016, p. 701-711
4.MESBAHI, T., OUARI, A., GHENNAM, T., BERKOUK, E.M., RIZOUG, N., MESBAHI, N., MERADJI, M., Renewable and Sustainable Energy Reviews, **40**, 2014, p. 204-213
5.DENG, D., Energy Science & Engineering, **3**, no. 5, 2015, p. 385-418
6.BATTKE, B., SCHMIDT, T.S., GROSSPIETSCH, D., HOFFMANN, V.H., Renewable and Sustainable Energy Reviews, **25**, 2012, p. 240–250
7.ABADA, S., MARLAIR, G., PETIT, A.L.M., SAUVANT-MOYNOT, V., HUET, F., Journal of Power Sources, **306**, 2016, p. 178–192
8.CABRERA-CASTILLO, E., NIEDERMEIER, F., JOSSEN, A., Journal of Power Sources, **324**, 2016,p. 509–520
9.SAHRAEI, E., BOSCO, E., DIXON, B., LAI, B., Journal of Power Sources, **319**, 2016, p. 56–65
10.KWON, N.H., Solid State Sciences **21**, 2013, p. 59-65
11.WU, B., WANG, J., LI, J., LIN, W., HU, H., WANG, F., ZHAO, F., GAN, C., ZHAO, J., Electrochimica Acta, **209**, 2016, p. 315–322
12.ZHANG, L., MA, Y., CHENG, X., DU, C., GUAN, T., CUI, Y., SUN, S., ZUO, P., GAO, Y., YIN, G., Journal of Power Sources, **293**, 2015, p. 1006–1015
13.CHEN, J., WANG, S., WHITTINGHAM, M.S., J. Power Sources, **174**, 2007, p. 442-448
14.CHEN, J., WHITTINGHAM, M.S., Electrochem. Commun., **8**, 2006, p. 855–858
15.FOTOUHI, A., AUGER, D.J., PROPP, K., LONGO, S., WILD, M., Renewable and Sustainable Energy Reviews, 56, 2016, p. 1008–1021
16.MOTE, V.; PURUSHOTHAM, Y.; DOLE, B., Journal of Theoretical and Applied Physics, **6**, no. 1, 2012, p. 1-8

Manuscript received: 19.07.2017